Critical viscosity exponent for fluids: Effect of the higher loops

Palash Das and Jayanta K. Bhattacharjee
Department of Theoretical Physics, Indian Association for the Cultivation of Science, Jadavpur, Kolkata 700 032, India
(Received 12 September 2002; published 10 March 2003)

We arrange the loopwise perturbation theory for the critical viscosity exponent x_η, which happens to be very small, as a power series in x_η itself, and argue that the effect of loops beyond two is negligible. We claim that the critical viscosity exponent should be very closely approximated by $x_\eta=(8/15\pi^2)(1+8/3\pi^2)\simeq 0.0685$.

DOI: 10.1103/PhysRevE.67.036103 PACS number(s): 64.60.Ht, 62.10.+s

Critical exponents, amplitude ratios, and scaling functions were issues of considerable importance three decades ago. Sophisticated calculations and experiments were carried out, which clearly established the correctness of the various theoretical models (Landau-Ginzburg equations for statics, and the various models of dynamics [1–4] introduced by Hohenberg and co-workers). Basically, the exponents could be classified into two types: (i) large exponents, i.e., exponents of $O(1)$ and (ii) small exponents, i.e., exponents of $O(0.1)$ or even smaller. It is the small exponents where the most crucial confrontation between theory and experiment can occur. That is why even after three decades, the small exponents remain an interesting issue. In static critical phenomena [5] the small exponents are associated with the critical correlation function at the transition point (η, the anomalous dimension exponent) and specific heat (α, the specific-heat exponent, the specific heat at constant volume for the liquid-gas transition and the specific heat at constant pressure for the superfluid transition of He^4), while in the critical dynamics the small exponent is associated with the shear viscosity. Accurate determination [6] of α for the superfluid transition and comparison with very detailed calculations [7] confirm the theoretical expectation. For the shear viscosity exponent z_η, the recent measurements [8] in the space shuttle have yielded an accurate value, namely, $z_\eta=0.0690\pm 0.0006$. The theoretical self-consistent two-loop calculation in $D=3$ of Hao yields $z_\eta=0.066\pm 0.002$, amazingly close to the experimental value. This raises the immediate question: What happened to the higher loops? The one-loop answer is 20% away from the experimental answer, the two-loop calculation produces the 20% enhancement almost entirely, and so what happens to the infinite number of loops that have been left out? This is the question that we address in the paper, and provide insight into why the higher loops happen to be unimportant.

In a liquid-gas system near the critical point or a binary liquid mixture near the critical mixing point, the order parameter ϕ is the density (concentration) difference and relaxes when disturbed from equilibrium according to the Langevin equation

$$\frac{\partial\phi(\vec{k})}{\partial t}=-\Gamma k^2(k^2+\kappa^2)\phi(\vec{k})+N(\vec{k}), \tag{1}$$

where $\phi(\vec{k})$ is the Fourier transformation of the D-dimensional field $\phi(x_1,\ldots,x_D)$. In the relaxation rate, the factor k^2 indicates that $\phi(\vec{x})$ is conserved. Γ is the Onsager coefficient [9–12] and the diffusion constant is $D=\Gamma/\chi$, where χ is the susceptibility. Near the critical point the susceptibility is $\chi=(k^2+\kappa^2)^{-1}$ with $\kappa=\xi^{-1}$, the inverse correlation length that diverges near $T=T_c$ as $\xi\propto|T-T_c|^{-\nu}$. The term N is a stochastic forcing that comes from the short wavelength modes. Fluctuation dissipation holds and the correlation of N is related in the usual way to the dissipation.

In a fluid, the density (concentrations) fluctuations will be affected by the velocity fluctuations and the effect of the velocity is to advect the concentration field, so that

$$\frac{\partial\phi(\vec{k})}{\partial t}+ik_\alpha\sum_{\vec{p}}\ v_\alpha(\vec{p})\phi(\vec{k}-\vec{p}) =-\Gamma k^2(k^2+\kappa^2)\phi(\vec{k})+N(\vec{k}). \tag{2}$$

The fact that the velocity fluctuations affect the concentration means that we need to know the velocity fluctuations. The equation of motion (for small fluctuation) is Navier-Stokes equation

$$\frac{\partial v_\alpha(\vec{k})}{\partial t}=-\eta k^2 v_\alpha(\vec{k})+N_\alpha^v(\vec{k}). \tag{3}$$

Note that v_α and N_α are solenoidal. However Eqs. (2) and (3) do not conserve the local free energy density $\Sigma_{\vec{k}}[(k^2+\kappa^2)\phi(\vec{k})\phi(-\vec{k})+v(\vec{k})v(-\vec{k})]$ when the dissipation terms are omitted, and consequently Eq. (3) needs to be argumented as

$$\frac{\partial v_\alpha(\vec{k})}{\partial t}+i\sum_{\vec{p}}\ p^2p_\beta T_{\alpha\beta}(\vec{k})\phi(\vec{p})\phi(\vec{k}-\vec{p}) =-\eta k^2 v_\alpha(\vec{k})+N_\alpha^v(\vec{k}), \tag{4}$$

where $T_{\alpha\beta}(k)=\delta_{\alpha\beta}-k_\alpha k_\beta/k^2$, the projection operator. The effect of the nonlinear terms in Eqs. (4) and (5) is to renormalize the Onsager coefficient Γ and the shear viscosity η. Dropping the nonlinear terms, we get the zeroth-order solution

$$\phi^{(0)}(\vec{k},t)=\int e^{-\Gamma k^2(k^2+\kappa^2)(t-t')}N(t')dt' \tag{5}$$

and

$$v_\alpha^{(0)}(\vec{k},t)=\int e^{-\eta k^2(t-t')}N_\alpha(t')dt'. \tag{6}$$

The first-order solution is easily seen to be

$$\phi^{(1)}(\vec{k},t)=-\int e^{-\Gamma k^2(k^2+\kappa^2)(t-t')}ik_\alpha\sum_{\vec{p}} v_\alpha^{(0)} \times(\vec{p},t')\phi^{(0)}(\vec{k}-\vec{p},t')dt' \tag{7}$$

and

$$v_\alpha^{(1)}(\vec{k},t)=-i\int e^{-\eta k^2(t-t')}p^2p_\beta\phi^{(0)} \times(\vec{p},t')\phi^{(0)}(\vec{k}-\vec{p},t')dt'. \tag{8}$$

The fields being stochastic in nature, the effect of the nonlinear terms in Eqs. (2) and (4) are to be understood as averaged over the noise terms, and it is easy to see that the nonlinear terms in Eq. (2) yield a term of the form $-k^2(k^2+\kappa^2)\int\Gamma^{(R)}(\vec{k},t-t')\phi^{(0)}(-\vec{k},t')dt'$ and those in Eq. (4) give $-k^2\int\eta^{(R)}(\vec{k},t-t')v_\alpha^{(0)}(-\vec{k},t')dt'$, when we split the quadratically nonlinear term as one field at zeroth order and the other at first order. For Eq. (2), this implies writing the nonlinear term as $ik_\alpha[\langle\Sigma_{\vec{p}}v_\alpha^{(0)}(\vec{p})\phi^{(1)}(\vec{k}-\vec{p})\rangle+\langle\Sigma_{\vec{p}}v_\alpha^{(1)}(\vec{p})\phi^{(0)}(\vec{k}-\vec{p})\rangle]$ and similarly for Eq. (4). This is exactly equivalent to a one-loop result. The two-loop results come from all the pairings of three, the three-loop results from the pairings of five and so on. The Fourier transforms $\Gamma^R(\vec{k},\omega)$ and $\eta^R(\vec{k},\omega)$ of $\Gamma^R(\vec{k},t-t')$ and $\eta^R(\vec{k},t-t')$ are the renormalized Onsager coefficient and the shear viscosity, respectively.

The renormalized transport coefficients $\Gamma^{(R)}(k,\omega)$ and $\eta^{(R)}(k,\omega)$ diverge at the critical point in the zero-frequency zero-wavelength limit and dominate the molecular contributions. From now on we will refer to these as $\Gamma(k,\omega)$ and $\eta(k,\omega)$. A little algebra shows that at one loop, we get the standard results [$\eta(k)k^2\gg\Gamma(k)k^2(k^2+\kappa^2)$]

$$\Gamma(k,\kappa)=\frac{1}{C_3}\int\frac{d^3p}{(p^2+\kappa^2)}\frac{\sin^2\theta}{\eta(\vec{k}-\vec{p})(\vec{k}-\vec{p})^2} \tag{9}$$

and

$$\eta(k,\kappa)=\frac{1}{4C_3}\int\frac{d^3p}{(p^2+\kappa^2)(p'^2+\kappa^2)} \times\frac{p^2(p^2-p'^2)^2\sin^2\theta}{[p^2(p^2+\kappa^2)\Gamma(\vec{p})+p'^2(p'^2+\kappa^2)\Gamma(\vec{p'})]}, \tag{10}$$

where $\vec{p'}=\vec{k}-\vec{p}$.

We now introduce the scaling behavior (long-wavelength divergence at the critical point) at $\kappa=0$ as

$$\Gamma(k)=\Gamma_0k^{-1+x_\eta}, \tag{11}$$

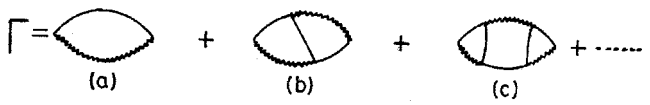

FIG. 1. Diagrammatic loop expansion for one- and two-loop diagrams for the density relaxation rate. The solid lines stand for density fluctuation and the wavy lines for velocity fluctuation.

$$\eta(k)=\eta_0k^{-x_\eta}k^2, \tag{12}$$

consistent with Eqs. (9) and (10), where x_η is the exponent that is yet unknown. Working at $\kappa=0$ in Eq. (9), we find

$$\eta_0\Gamma_0=\frac{\pi^2}{8}+O(x_\eta). \tag{13}$$

We anticipate at this stage that x_η is very small and are going to use it as a small parameter in setting up our calculation. Our main observation is that a loopwise expansion can be cast as an expansion in powers of x_η for the quantity $\eta_0\Gamma_0$. We can get yet another expansion for $\eta_0\Gamma_0$ by using Eq. (10) at $\kappa=0$. The integral has a long-wavelength divergence at $x_\eta=0$ and this leads to the evaluation of the integral as a pole in x_η. This yields

$$\eta_0\Gamma_0=\frac{1}{15x_\eta}+O(1). \tag{14}$$

Combining Eqs. (13) and (14),

$$x_\eta=\frac{8}{15\pi^2} \tag{15}$$

to the lowest order.

We now observe that the perturbation theory for Γ and η can be expressed through diagrams as shown in Figs. 1 and 2, with a wavy line denoting the velocity field (propagator or correlator as the case may be) and a solid line denoting the density field.

For higher loops, self-energy insertion [13–15] are not shown separately. They are handled by a finite frequency evaluation of a lower loop and yield insignificant corrections. The important graphs are the vertex correction varieties [16] that are shown in Figs. 1 and 2. If we compare a one-loop and a two-loop graph, we note that compared to the one-loop graph, the two-loop graph has two additional time zones: one dominated by viscosity relaxation, the other lacking any viscosity contribution. This means an additional factor of $(\eta_0\Gamma_0)^{-1}$ everytime a loop increases. Now, in addition, we note that for every loop the viscosity graphs diverge logarithmically if $x_\eta=0$ and have a pole for small x_η. We simply

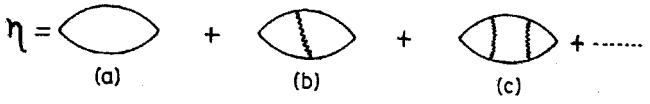

FIG. 2. Diagrammatic loop expansion for one- and two-loop diagrams for the viscosity. The solid lines stand for density fluctuation and the wavy lines for velocity fluctuation.

need to evaluate this pole in a manner very similar to the dimensional regularization scheme in field theory. From Fig. 1, there emerges

$$\eta_0\Gamma_0 = J_1 + \frac{1}{\eta_0\Gamma_0}J_2 + \frac{1}{(\eta_0\Gamma_0)^2}J_3 + \cdots, \tag{16}$$

while from Fig. 2, we get

$$\eta_0\Gamma_0 = \frac{I_1}{x_\eta} + \frac{I_2}{\eta_0\Gamma_0 x_\eta} + \frac{I_3}{(\eta_0\Gamma_0)^2 x_\eta} + \cdots, \tag{17}$$

where I_n and J_n are integrals corresponding to diagrams with n loops. Figures 1(a) and 2(b) show the one-loop integrals corresponding to Eqs. (9) and (10). The integrals corresponding to the two-loop diagrams [Figs. 1(b) and 2(b)] are

$$k^2 I_2 = \frac{1}{2}\int \frac{d^3p}{C_3}\int \frac{d^3q\, p_\alpha T_{\alpha\beta}(k) q_\beta p_\mu T_{\mu\nu}(k-p-q) q_\nu [p^2-(\vec{k}-\vec{p})^2][q^2-(\vec{k}-\vec{q})^2]}{p^2 q^2 (\vec{k}-\vec{p}-\vec{q})^2 [p^3+(\vec{k}-\vec{p})^3][q^3+(\vec{k}-\vec{q})^3]}, \tag{18}$$

$$J_2 = \int \frac{d^3p}{C_3}\int \frac{d^3q}{C_3} \frac{[(\vec{k}-\vec{p}-\vec{q})^2-(\vec{k}-\vec{p})^2][(\vec{k}-\vec{p}-\vec{q})^2-(\vec{k}-\vec{q})^2]}{(\vec{k}-\vec{p})^2(\vec{k}-\vec{q})^2(\vec{k}-\vec{p}-\vec{q})^2} \frac{k_\alpha T_{\alpha\beta}(p)(\vec{k}-\vec{q})_\beta k_\mu T_{\mu\nu}(q)(\vec{k}-\vec{p})_\nu}{p^2 q^2 [(\vec{k}-\vec{p})^3+(\vec{k}-\vec{q})^3+(\vec{k}-\vec{p}-\vec{q})^3]}. \tag{19}$$

Using Eq. (14) to substitute for $\eta_0\Gamma_0$ in Eqs. (16) and (17), we end up with

$$\eta_0\Gamma_0 = J_1 + 15x_\eta J_2 + (15x_\eta)^2 J_3 + \cdots. \tag{20}$$

The important fact is that $15x_\eta J_2 \ll 1$ and this trend continues through higher loops. This fixes $\eta_0\Gamma_0$.

Turning now to the diagrams of Fig. 2, they lead to [using Eq. (14) repeatedly]

$$\begin{aligned}\eta_0\Gamma_0 &= \frac{I_1}{x_\eta} + 15I_2 + x_\eta(15)^2 I_3 + \cdots \\ &= \frac{I_1}{x_\eta}\left[1 + 15x_\eta\frac{I_2}{I_1} + x_\eta(15)^2 x_\eta\frac{I_3}{I_1} + \cdots\right] \\ &= \frac{1}{15x_\eta}\left[1 + \frac{8}{\pi^2} + x_\eta\frac{8}{\pi^2}\frac{15I_3}{I_1} + x_\eta^2\frac{8}{\pi^2}\frac{15^2 I_4}{I_1} + \cdots\right],\end{aligned} \tag{21}$$

leading to the ordering in x_η. The calculation of I_2/I_1 yields $\frac{1}{3}$ and hence to two-loop order,

$$x_\eta = \frac{8}{15\pi^2}\left(1 + \frac{8}{3\pi^2}\right) \simeq 0.0685. \tag{22}$$

The reason why I_2 is smaller than I_1 has to do with the projection factors that yield zeros in the integrand. The large number of zeros and their distributions in the three loop integral lead to I_3/I_1 being significantly smaller than $\frac{1}{10}$. The additional factor of x_η now makes the three-loop contribution negligible. The important point is that for a n-loop integral I_n, the projection factor produces sufficient cancellation, so that $15^{n-2}I_n$ is always $O(1)$, and this ensures that higher loops produce insignificant corrections when $x_\eta \ll 1$. This is the crucial point of the paper. The thing that one needs to appreciate is that $I_2 < I_1$, but $I_3 \ll I_1$. What we will try to elucidate is the reason behind this change. Unfortunately this reason is not a universal feature. It is specific to this problem. The combination of projection operators associated with the transverse velocity field makes the three-loop integrals small, and this combination is maintained in the subsequent loops. It should be pointed out that this does not imply that this will make an asymptotic series convergent. As in all loop expansions in critical phenomena, this expansion in x_η too is an asymptotic expansion. What the smallness of the loop integrals does is that it postpones the onset of the divergent behavior to a higher order. This implies that the effect of the higher loops will be muted and the agreement between a two-loop result and experiment will be better than expected.

The generic form of the three-loop graph of Fig. 2(c) involves a few different time orderings, all of which are shown in Fig. 3. A typical contribution $I_3^{(1)}$ coming from the last two graphs of Fig. 3 is

$$\begin{aligned}k^2 I_3^{(1)} = -\int \frac{d^3p}{C_3}\frac{d^3q}{C_3}\frac{d^3r}{C_3} &\frac{[(\vec{k}-\vec{p})^2-p^2][(\vec{k}-\vec{r})^2-r^2]}{(\vec{k}-\vec{p})^2(\vec{k}-\vec{q})^2} \\ &\times \frac{p_\alpha T_{\alpha\beta}(k) r_\beta p_\mu T_{\mu\nu}(p-q) p_\nu}{(\vec{k}-\vec{r})^2[p^3+|\vec{p}-\vec{k}|^3][q^3+|\vec{k}-\vec{q}|^3]} \\ &\times \frac{q_\gamma T_{\gamma\lambda}(q-r) q_\lambda}{[r^3+|\vec{k}-\vec{r}|^3](\vec{k}-\vec{p}-\vec{q})^2(\vec{k}-\vec{q}-\vec{r})^2}.\end{aligned} \tag{23}$$

The evaluation of I_3 has to be in the limit of $k \to 0$. This allows us to drop k from all the terms after a factor of k^2 has been extracted from the integral. We now carry out the following steps in a D-dimensional space for generality

(a) Expand the number in powers of k^2 and keep the first term (this is proportional to k^2), and set $k=0$ everywhere else.

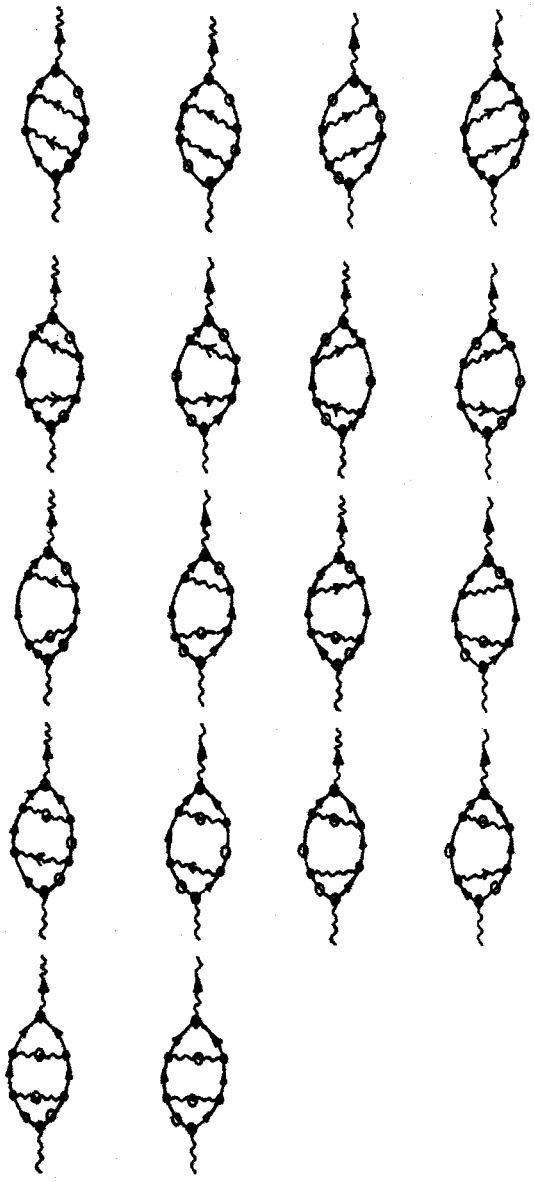

FIG. 3. Three-loop diagrams of the vertex correction variety for the viscosity, showing all possible time orderings. Propagators appear with an arrow and correlators with an open circle.

(b) Perform an angular average over the directions of $\vec{k}$.

In a D-dimensional space, $I_3^{(1)}$ after some long algebra reduces to

$$I_3^{(1)} = -\frac{1}{4D(D+2)} \int d^D p\, d^D q\, d^D r \times \frac{[D(\vec{p}\cdot\vec{r})^2 - p^2 r^2]}{r^4 (\vec{q}-\vec{r})^4 (\vec{p}-\vec{q})^4} \times \frac{[p^2 q^2 - (\vec{p}\cdot\vec{q})^2][q^2 r^2 - (\vec{q}\cdot\vec{r})^2]}{p^D q^D r^D}. \quad (24)$$

It is the factor $(\vec{p}\cdot\vec{r})^2 - p^2 r^2/D$ that is qualitatively new, to the best of our knowledge. The two-loop integral I_2 did not have such a factor. The characteristic feature of this factor is that in the absence of the quite indirect additional appearance of the angle between $\vec{p}$ and $\vec{r}$ because of the term $|\vec{q}-\vec{r}|^4$ and $|\vec{p}-\vec{q}|^4$ in the denominator, the averaging over the directions of $\vec{r}$ (or $\vec{p}$) would make $I_3^{(1)}$ identically zero. In practice, this effect makes it unusually small compared to I_2 or I_1, which do not have such a factor. If we look at the higher loops, each additional loop brings in a factor of this type, and that is the reason behind the successive diminishing of each of these integrals.

A numerical evaluation in $D=3$ yields $I_3^{(1)} \simeq -(\frac{1}{15})^2$, which makes the point that we wanted to make. The corrections from the three-loop graphs are down by an order of x_η and this effect persists to higher orders. This is the reason why the two-loop calculation of the viscosity exponent gives an answer surprisingly close to the experimental value.

In closing we would like to mention that we have used a Gaussian free energy in this calculation. There is a quartic part in the free energy which is responsible for the anomalous dimension η. The correction coming from this is once again largest at the loop level when it first appears. There are no genuine three-loop graphs involving only the quartic term in the expansion shown in Eq. (17). In the expansion of Eq. (16), J_3 involves a combination of two four-point and two three-point vertices. It should be noted that J_2 already plays a negligible role. Consequently, it is not necessary to take J_3 into account. The net result is that from one to two loops, there is a substantial change in x_η, but thereafter the contribution of the higher loops are ordered by x_η itself, and with the integrals themselves quite small, the small value of x_η ensures that the higher-loop effects are small.

[1] K. Kawasaki, Ann. Phys. (N.Y.) **61**, 1 (1970).

[2] T. Ohta and K. Kawasaki, Prog. Theor. Phys. **55**, 1384 (1976).

[3] R.A. Ferrell, Phys. Rev. Lett. **24**, 1169 (1970).

[4] E.D. Siggia, B.I. Halperin, and P.C. Hohenberg, Phys. Rev. B **13**, 2110 (1976).

[5] See, e.g., J.V. Sengers and J.M.H. Levelt Sengers, Annu. Rev. Phys. Chem. **37**, 189 (1986).

[6] C. Bagnuls and C. Bervillier, Phys. Rev. B **32**, 7209 (1989); also see V. Dohm, J. Low Temp. Phys. **69**, 51 (1987); R. Schloms and V. Dohm, Europhys. Lett. **3**, 413 (1987).

[7] J.A. Lipa, D.R. Swanson, J.A. Nisen, T.C.P. Chui, and U.E. Israelson, Phys. Rev. Lett. **76**, 944 (1996).

[8] R.F. Berg, M.R. Moldover, and G.A. Zimmerli, Phys. Rev. Lett. **82**, 920 (1999).

[9] R.F. Berg, M.R. Moldover, and G.A. Zimmerli, Phys. Rev. E **60**, 4079 (1999).

[10] H. Hao, Ph.D. thesis, University of Maryland, 1991 (unpublished).

[11] R. Folk and G. Moser, Phys. Rev. E **57**, 683 (1998); see also **57**, 705 (1998).
[12] G. Flossmann, R. Folk, and G. Moser, Phys. Rev. E **60**, 779 (1999); and see also Int. J. Thermophys. **22**, 89 (2001).
[13] J.K. Bhattacharjee and R.A. Ferrell, Phys. Lett. **27A**, 290 (1980).
[14] J.K. Bhattacharjee and R.A. Ferrell, Phys. Rev. A **23**, 1511 (1981).
[15] J.K. Bhattacharjee and R.A. Ferrell, Phys. Rev. A **27**, 1544 (1983).
[16] P. Das and J.K. Bhattacharjee, Phys. Rev. E **63**, 020202(R) (2001).